Journal of Cerebral Blood Flow & Metabolism (2010) 30, 211–221

www.jcbfm.com

Altered brain mitochondrial metabolism in healthy aging as assessed by *in vivo* magnetic resonance spectroscopy

Fawzi Boumezbeur[1,2], Graeme F Mason[1,3], Robin A de Graaf[1,4], Kevin L Behar[1,3], Gary W Cline[5], Gerald I Shulman[5,6,7], Douglas L Rothman[1,4] and Kitt F Petersen[5]

[1]*Department of Diagnostic Radiology, Yale School of Medicine, New Haven, Connecticut, USA;* [2]*Neurospin, I2BM, CEA, Gif-sur-Yvette, France;* [3]*Department of Psychiatry, Yale School of Medicine, New Haven, Connecticut, USA;* [4]*Department of Biomedical Engineering, Yale School of Medicine, New Haven, Connecticut, USA;* [5]*Department of Internal Medicine, Yale School of Medicine, New Haven, Connecticut, USA;* [6]*Department of Cellular and Molecular Physiology, Yale School of Medicine, New Haven, Connecticut, USA;* [7]*Howard Hughes Medical Institute, Yale School of Medicine, New Haven, Connecticut, USA*

A decline in brain function is a characteristic feature of healthy aging; however, little is known about the biologic basis of this phenomenon. To determine whether there are alterations in brain mitochondrial metabolism associated with healthy aging, we combined $^{13}C/^{1}H$ magnetic resonance spectroscopy with infusions of [1-^{13}C]glucose and [2-^{13}C]acetate to quantitatively characterize rates of neuronal and astroglial tricarboxylic acid cycles, as well as neuroglial glutamate–glutamine cycling, in healthy elderly and young volunteers. Compared with young subjects, neuronal mitochondrial metabolism and glutamate–glutamine cycle flux was ~30% lower in elderly subjects. The reduction in individual subjects correlated strongly with reductions in *N*-acetylaspartate and glutamate concentrations consistent with chronic reductions in brain mitochondrial function. In elderly subjects infused with [2-^{13}C]acetate labeling of glutamine, C4 and C3 differed from that of the young subjects, indicating age-related changes in glial mitochondrial metabolism. Taken together, these studies show that healthy aging is associated with reduced neuronal mitochondrial metabolism and altered glial mitochondrial metabolism, which may in part be responsible for declines in brain function.

Journal of Cerebral Blood Flow & Metabolism (2010) **30,** 211–221; doi:10.1038/jcbfm.2009.197; published online 30 September 2009

Keywords: aging; human brain; metabolism; mitochondria; ^{13}C MRS; ^{1}H MRS

Introduction

Normal human aging is associated with a decline in brain function, including cognitive, memory, and sensory processes (Hedden and Gabrieli, 2004). Alterations in mitochondrial function have been implicated in age-related neurodegenerative diseases through reactive oxygen species hypothesis and have been suggested to have a role in the loss of brain function with healthy aging (Reddy, 2007). However, direct evidence of impaired mitochondrial function has not been shown. Studies using positron emission tomography (PET) have shown decreases in brain glucose metabolism associated with aging (Salat *et al*, 2004; Kalpouzos *et al*, 2009), but these may not be related to mitochondrial changes. Furthermore, it is unclear whether the decreases are due to changes at the cellular level or are secondary to brain shrinkage (Ibáñez *et al*, 2006).

Over the past decade, advances in magnetic resonance spectroscopy (MRS) by several groups have provided direct noninvasive measurements of metabolic fluxes in the healthy human brain (for reviews, see Shen and Rothman, 2002; Hyder *et al*, 2006; Mangia *et al*, 2009) and have been applied to studies of patients with neurodegenerative disorders (Lin *et al*, 2003). Of particular interest in this regard

Correspondence: Professor DL Rothman and KF Petersen, Yale University School of Medicine, 333 Cedar Street, PO Box 208020, New Haven, CT 06520-8020, USA.
E mail: douglas.rothman@yale.edu
This study was supported by UPHS Grant nos R01 NS-037527 (DLR), K02 AA-13430 (GFM), R01 AG-23686 (KFP), and P01 DK-68229 (KFP, DLR, GIS), Howard Hughes Medical Institute (GIS), The Keck Foundation, and a CTSA award (14L1 RR024139) from the NIH to the Yale School of Medicine.
Received 4 June 2009; revised 28 July 2009; accepted 14 August 2009; published online 30 September 2009

is the recent development of ^{13}C MRS methods, in combination with selectively ^{13}C-labeled precursors, to measure individual rates of neuronal (V_{TCAn}) and glial (V_{TCAg}) mitochondrial energy production, as well as the rate of the glutamate–glutamine cycle—a measure of neurotransmitter glutamate release (V_{cycle}). In these studies, we applied these novel ^{13}C MRS methods to directly determine whether the rates of neuronal and glial tricarboxylic acid (TCA) cycle flux, which are a direct measure of mitochondrial function, are altered in the brain of healthy, elderly subjects compared with young control subjects.

Materials and methods

Subjects

Seven healthy, nonsmoking elderly (2 women/5 men; aged: 76 ± 8 years, body mass index: $24 \pm 3\,kg/m^2$) and eight young (3 women/5 men; aged: 26 ± 7 years, body mass index: $23 \pm 4\,kg/m^2$) volunteers were studied. All subjects underwent a complete medical history and physical examination along with blood tests to verify their normal blood and platelet counts, electrolytes, AST (aspartate transaminase), ALT (alanine transaminase), urea nitrogen, creatinine, cholesterol, and triglycerides. All subjects (both young and elderly) were in excellent health, nonsmoking, and were free of any significant chronic diseases that might impact brain metabolism, including diabetes, hepatic, renal, cardiovascular, and pulmonary conditions, hypertension, mental disorders, and joint disease. This was determined by medical history and physical examination, including blood screens and electrocardiogram. None of the subjects took any medications, except the young female subjects who took birth control pills. Before enrollment, all subjects underwent a 75-g, 3-h oral glucose tolerance test (OGTT) to verify normal glucose tolerance defined as a fasting plasma glucose level >80 and <100 mg/dL and a mean plasma glucose concentration level ≤ 140 mg/dL at 120 mins and normal $HgbA_1$ ($<6\%$). No subject showed evidence for previous ischemic episodes or clinically relevant brain shrinkage in the quantitative gray–white–cerebrospinal fluid (CSF) magnetic resonance imaging (MRI) that was part of the scanning procedure (see Figure 1). All subjects had correctable vision and were able to view the projection screen.

Each subject participated in two MRS studies: (1) hyperglycemia with administration of [1-^{13}C]glucose and (2) during [2-^{13}C]acetate administration. The studies were conducted in random order. The subjects were admitted in the morning after an overnight fast; two antecubital intravenous lines were inserted, i.e., one for infusion and the other for blood collection. The subjects were positioned within the magnet and after acquisition optimization and collection of baseline ^{13}C spectrum, either [1-^{13}C]glucose or [2-^{13}C]acetate was infused. During both experiments, the subjects were awake with their eyes open and were watching a slide show presentation of neutral nature pictures during the study.

For glucose experiments, a primed-variable rate infusion of [1-^{13}C]glucose was administered (1.1 mmol/L of 99% APE (Atom Percent Enrichment), Cambridge Isotopes, Cambridge, MA, USA) to increase plasma glucose concentrations to 180 mg/dL and maintain this for 120 mins. For acetate experiments, [2-^{13}C]acetate was administered (350 mmol/L sodium salt of 99% ^{13}C APE, Sigma-Aldrich, Miamisburg, OH, USA) as a primed-continuous infusion of 3.0 mg/kg per min for the 120-min study duration (Shen *et al*, 1999; Lebon *et al*, 2002). Blood samples were collected for every 5 to 10 mins for determining plasma glucose and acetate APE, as well as for concentrations of plasma glucose and lactate. Plasma glucose and lactate concentrations were measured using an YSI STAT 2300 Analyzer (Yellow Springs Instruments, Yellow Springs, CA, USA). Fractional enrichments and distribution of ^{13}C label among the six glucose carbon atoms were determined by gas chromatography-mass spectroscopy as described previously (Mason *et al*, 2007).

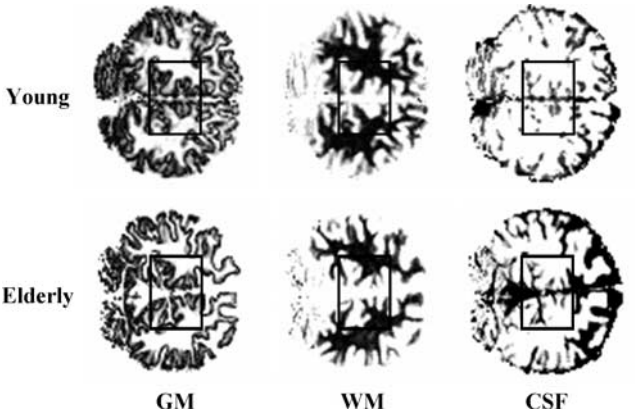

Figure 1 Typical position of the spectroscopic volume of interest (~ 100 mL) and brain segmentation into gray matter (GM, left), white matter (WM, center), or cerebral spinal fluid (CSF, right) from two healthy young (top) and elderly volunteers (bottom). In spite of the overall brain atrophy in the elderly subjects, the proportion of gray and white matter in the volumes of interest was similar (Young: $\%GM = 47 \pm 1\%$ versus Elderly: $\%GM = 49 \pm 2\%$).

$^{13}C/^{1}H$ Magnetic Resonance Spectrometry Acquisition

Magnetic resonance spectrometry data were acquired on a 4.0-T whole-body magnet interfaced to a Bruker AVANCE Spectrometer (Bruker Instruments, Billerica, MA, USA). Subjects were placed supine within the magnet, with their heads immobilized with foam and lying on top of a radiofrequency probe consisting of one ^{13}C circular coil (8.5 cm in diameter) and two ^{1}H quadrature coils for acquisition and decoupling. Volumes of interest (~ 100 mL) were centered in the midline occipito-parietal lobe. After tuning, acquisition of scout images, shimming with the FASTERMAP procedure, and calibration of decoupling power, ^{13}C spectra were acquired before and during the ^{13}C-labeled substrate infusion using a localized adiabatic ^{13}C-[^{1}H]-refocused INEPT sequence optimized for glutamate and glutamine-C4 using 3D-ISIS combined with

outer volume saturation for the localization of ^{1}H magnetization (Shen *et al*, 1999) (128 transients, TR (repetition time) = 2.5 secs, 5.3 mins time resolution). The spectroscopic volume was located in the occipital–parietal lobe, with the size adapted to each volunteer (Young (N = 8): 97.6 ± 2.5 mL and Elderly (N = 7): 97.4 ± 1.6 mL, respectively).

^{1}H spectra were acquired under the exact same conditions using a ^{1}H radiofrequency probe (7 cm in diameter) and a phase-encoding LASER-POCE sequence (FOV (field of view) = 16 cm, 16 steps, 16 transients, TR = 3.5 secs, TE (echo time) = 42 msecs) (Marjanska *et al*, 2004). A reference spectrum and a double-inversion metabolite-nulled spectrum (TI_1 = 1.7 secs, TI_2 = 0.54 secs) were acquired from the same volume of interest (Barker *et al*, 1994; Behar *et al*, 1994). The spectroscopic volume was located in the occipital–parietal lobe (Elderly (N = 7): 26.4 ± 0.9 mL).

Data Processing

Magnetic Resonance Imaging Segmentation: The tissue composition of each voxel was determined from T_1-based image segmentation maps as described previously (Mason and Rothman, 2002). Briefly, sets of B_1 maps and inversion-recovery images were acquired and processed to yield quantitative T_1 and proton density maps, which were converted to segmented images of gray matter, white matter, and CSF (see Figure 1).

^{1}H Spectra Analysis

All ^{1}H spectra were analyzed using an LCModel 6.1 (Provencher, 1993) (Stephen Provencher, Oakville, ON, Canada). The LCModel was generated by simulating spectra for every observable metabolite with Matlab 7.0 (The MathWorks, Natick, MA, USA) and SpinWizard (Bruker Analytik GmbH, Ettlingen, Germany) using published values of ^{1}H chemical shifts and homonuclear ^{1}H-^{1}H coupling constants (J_{HH}) obtained from Govindaraju *et al* (2000). After subtraction of an averaged macromolecule spectrum from the raw spectra, 1-Hz Gaussian apodization was applied before the LCModel analysis. Relative concentrations obtained from the LCModel were converted to absolute concentrations by reference to the endogenous water signal. The water content for each voxel was calculated using tabulated values of water content in gray matter (43.3 mol/L), white matter (35.9 mol/L), and CSF (55.0 mol/L) (Lentner, 1981). Corrections were applied for T_1 relaxation effects and proton density differences between the 'Young' and 'Elderly' cohorts on the basis of the individual T_1 and proton density maps of the brain (data not shown).

^{13}C Spectra Analysis

All ^{13}C spectra were also analyzed using LCModel 6.1 modified to process ^{13}C spectral data as explained by Henry *et al* (2003). The LCModel was generated by simulating spectra for every observable isotopomer with NMRSim 2.8 (Bruker Analytik GmbH, Ettlingen, Germany) using published values of ^{13}C chemical shifts and homonuclear ^{13}C-^{13}C coupling constants (J_{CC}) obtained from Henry *et al* (2003). The spectra were added three-by-three in running averages of 16 mins to increase the signal to noise ratio (SNR) before processing. A 3-Hz Gaussian apodization and zero filling to 8K data points were applied to all spectra before the LCModel analysis. Relative concentrations obtained from the LCModel were converted to absolute concentrations by reference to the natural abundance (1.1%) signal of *N*-acetylaspartate (NAA) carbon-3 assuming a NAA pool size of 11 μmol/g for 'Young' subjects on the basis of previous ^{13}C MRS measurements that performed natural abundance quantitation (Mason *et al* 2007). For the elderly subjects, measured NAA concentrations determined from ^{1}H MRS spectra were used. Calibration of the basis set to account for differences in polarization transfer efficiency and off-resonance effects were realized using a series of phantom experiments (data not shown). For the very first time points, because of the low signal-to-noise ratio, systematic overestimations were apparent. Therefore, peak heights were determined manually and scaled on the last spectrum. To improve sensitivity of the measurement, only singlet signals were considered for glutamate (Glu-C4, Glu-C3, and GluC-2) and glutamine (Gln-C4, Gln-C3, and Gln-C2). On the basis of probabilities of obtaining double- and triple-labeled isotopomers, correction factors were calculated and applied to account for the contribution of these isotopomers (Glu-C43, Glu-C32, Glu-C234, Gln-C43, Gln-C32, and Gln-C234).

Metabolic Modeling Analysis

Model Fitting to ^{13}C Time Courses and Metabolic Flux Determination: Previous labeling experiments have established that cerebral metabolism can be characterized by two distinct metabolic compartments associated with neurons and glial cells (see Lebon *et al*, 2002). Time courses of ^{13}C labeling for glutamate and glutamine in the C4, C3, and C2 positions from both [1-^{13}C]glucose and [2-^{13}C]acetate were fitted simultaneously according to this two-compartment metabolic model (Mason *et al*, 1995; Mason *et al*, 1999; Gruetter *et al*, 2001; Henry *et al*, 2006) using Matlab 7.0 (The MathWorks) and Cwave (Mason, 2003) with time courses for plasma acetate, lactate, and glucose concentrations, as well as ^{13}C fractional enrichments as input functions for each experiment. Values for rates of the glutamate–glutamine cycle (V_{cycle}) along with rates of neuronal and glial TCA cycles (noted as V_{TCAn} and V_{TCAg}, respectively) were adjusted iteratively using a simulated annealing algorithm. The mitochondrial–cytosolic glutamate–α-ketoglutarate exchange rate in neurons and astrocytes (V_{Xn} and V_{Xg}) were fitted to improve the accuracy of TCA cycle rates determination. Pyruvate carboxylase activity ($\boldsymbol{V_{PC}}$) was considered equal to 0.06 of V_{cycle} on the basis of the value reported previously by Mason *et al* (2007)after the infusion of [2-^{13}C]glucose in humans. For the young group, concentrations of glutamate and glutamine used for the modeling were assumed to be 9.1 and 4.1 μmol/g, respectively, on the basis of the values

reported by a previous MRS study of a similar volume (Mason *et al*, 2007). For the elderly group, glutamate and glutamine pools sizes considered were those given by the ^{1}H spectra analysis. Recently, the precision of using a two-compartment model to calculate metabolic fluxes has been evaluated numerically for a [1-^{13}C]glucose infusion (Shestov *et al*, 2007; Shen *et al*, 2009). High precision was found for the measurement of the neuronal TCA cycle, but there was lower precision for measuring the glutamate–glutamine cycle because of the product precursor relationship of glutamine from neuronal glutamate. To enhance the precision of determining glutamate–glutamine cycle flux as well as the glial TCA cycle, we conducted studies using [2-^{13}C]acetate (Lebon *et al*, 2002), which directly labeled the astrocytic glutamate and glutamine pool. For each subject, data from the glucose and acetate infusions were fitted simultaneously to obtain metabolic rates. In addition, the fraction of astrocytic glutamate as a fraction of the total was calculated from group data and found to be similar within the elderly and control subjects, and consistent with the previous report of Lebon *et al* (2002) of $\sim$7% of the total pool.

Previous *in vivo* studies have strongly suggested that the glutamate–glutamine cycle is the major pathway of neuronal glutamate repletion; however, other pathways are active in cell cultures. These pathways were not included in the modeling, because any flux of alternate glutamate precursors from the glia to neurons would be included in the [2-^{13}C]acetate measurement (Lebon *et al*, 2002). Several studies have shown that anaplerosis may have an important role in maintaining the glutamate–glutamine cycle, through replenishment of lost glutamate due to either glial oxidation or diffusion into the extra cellular fluid (ECF) (Gruetter *et al*, 2001; Lebon *et al*, 2002; Oz *et al*, 2004; Hyder *et al*, 2006; Mason *et al*, 2007). As labeling curves from the [1-^{13}C]glucose and [2-^{13}C]acetate precursors are not highly sensitive to the rate of anaplerosis, but are based on steady-state labeling from [1-^{13}C]glucose, the fractional rate of anaplerosis was similar between both the groups and would not impact the calculated fluxes significantly. To definitively address the question of whether anaplerosis is altered in aging would require either the use of [2-^{13}C]glucose as a precursor or obtaining time courses from [1-^{13}C]glucose with higher sensitivity to the C2 positions of glutamate and glutamine (Mason *et al*, 2007).

LCModel Analysis

Figure 1 in Supplementary material shows two steady-state spectra from the same young volunteer, obtained from (Supplementary Figure 1A) the last 15 mins of a 2-h [1-^{13}C]glucose or (Supplementary Figure 1B) the last 25 mins of a 2-h [2-^{13}C]acetate infusion, scaled to show the differences in the pattern of ^{13}C labeling between acetate and glucose infusions. As detailed, the multiple positions of glutamate, glutamine, and aspartate are well resolved with typical Cramer–Rao lower bounds values at the end of the study being below 5% for Glu-C4, below 15% for glutamate-C3, glutamine-C4, glutamate-C2, and aspartate-C3, and below 25% for NAA-C3, glutamine-C3, and glutamine-C2. To achieve a higher level of accuracy in the measurement of the NAA-C3 signal, ^{13}C labeling was assumed to be negligible during the first 60 mins, and all spectra were summed over this interval. In this manner, the Cramer–Rao lower bounds for the NAA-C3 peak was $<$15%. Figure 2 in Supplementary material shows a typical ^{1}H neurochemical profile acquired from one of the elderly volunteers (thick line) and its best fit by linear combination of spectra (thin line). The major metabolites (from top to bottom: NAA, glutamate + glutamine, creatinine, myoinositol, and choline) were determined with Cramer–Rao lower bounds below 5%. The average concentrations are given in Table 1B.

Metabolic Modeling and Flux Determinations

Figures 2A–2D show glutamate-C4, glutamate-C3 ([1-^{13}C]glucose infusion), and glutamine-C4, glutamine-C3 ([2-^{13}C]acetate infusion) experimental time courses, as well as the corresponding best fits obtained for a young and an elderly volunteer. The average values for $\boldsymbol{V}_{\mathrm{TCA}}$, V_{TCAn}, V_{TCAg}, and V_{cycle} for both groups are given in Table 1A. The value $V_{\mathrm{TCAg}}/\boldsymbol{V}_{\mathbf{TCA}}$ is also given and represents the contribution of the astroglia to overall brain oxidative energy metabolism.

Correlation Between Changes in Compartmentalized Metabolite Concentrations and Fluxes

Positive correlations were found between individual neuronal metabolite concentrations (NAA and glutamate) and flux rates (V_{TCAn}) (see Figures 3A and 3B, respectively), as well as between astroglial ones (myo-inositol and V_{TCAg}) (see Figure 3C) using Pearson's correlation coefficients.

Statistical Analysis

Statistical analyses were carried out using SysStat (Systat Software, San Jose, CA, USA). The statistical significance of differences between the young and elderly subjects, were performed using two-sample Bonferroni's *t*-tests. The correlation between neuronal and astroglial metabolites and fluxes in the elderly volunteers were calculated using Pearson's product–moment correlation coefficients (R). All data are presented as mean $\pm$ s.d.

Results

The MRS studies were carried out on a whole-body 4.0-T magnet (Bruker Instruments) from volumes of interest ($\sim$100 mL) centered in the midline occipito-parietal lobe of 15 healthy volunteers, 8 young (3 women and 5 men; aged: 26 $\pm$ 7 years, body mass index: 23 $\pm$ 4 kg/m^2; mean $\pm$ s.d.) and 7 elderly (2 women and 5 men; aged: 76 $\pm$ 8 years, body mass index: 24 $\pm$ 3 kg/m^2; mean $\pm$ s.d.) all of whom underwent separate [1-^{13}C]glucose and [2-^{13}C]acetate infusions. To match levels of wakefulness and visual

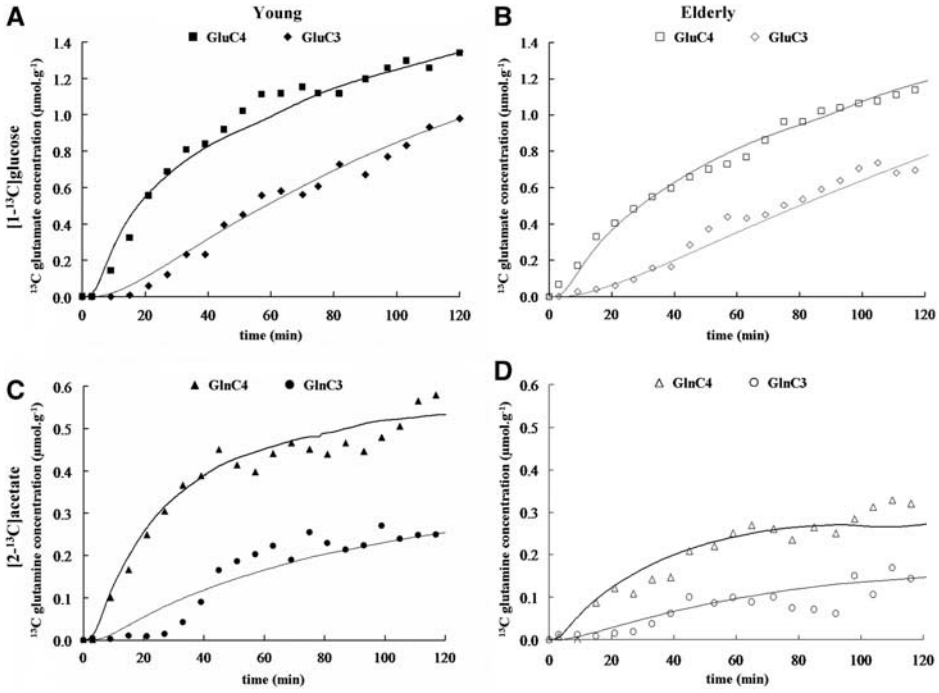

Figure 2 Time courses of glutamate (**A** and **B**) and glutamine (**C** and **D**) ^{13}C concentrations for C4 and C3 positions from one young (left, dark symbols) and one elderly (right, open symbols) volunteer during the infusion of [1-^{13}C]glucose (top) and during the infusion of [2-^{13}C]acetate (bottom). The corresponding best fits by the metabolic model are shown as solid lines through the data points. The scale for glutamine is adjusted to facilitate the visualization of the kinetics. Symbols: Glu-C4: squares (■ and □); Glu-C3: diamonds (◆ and ◇); Gln-C4: triangles (▲ and Δ); Gln-C3: circles. (○ and ●).

Table 1 Mean flux values (a) and metabolites pools sizes (b) for Young and Elderly subjects

(a) *(Mean ± s.d.)*	V_{TCA}	V_{TCAn}	V_{TCAg}	V_{cycle}	V_{TCAg}/V_{TCA}	V_{cycle}/V_{TCAn}
Young ($n=8$)	0.65 ± 0.03	0.53 ± 0.03	0.13 ± 0.01	0.16 ± 0.01	20 ± 1	0.32 ± 0.03
Elderly ($n=7$)	0.54 ± 0.04	0.38 ± 0.04	0.17 ± 0.01	0.13 ± 0.02	31 ± 2	0.34 ± 0.03
Difference	−17% ($P=0.04$)	−28% ($P=0.02$)	−30% ($P=0.02$)	−24% ($P=0.06$)	+ 58% ($P=10^{-3}$)	+ 7% ($P=0.56$)
(b) *(Mean ± s.d.)*	*NAA*	*Glu*	*Ins*	*Gln*	*Cho*	*Cr*
Young ($n=7$)	10.8 ± 0.6	8.9 ± 0.8	7.5 ± 1.0	3.7 ± 0.6	1.5 ± 0.1	8.3 ± 0.7
Elderly ($n=7$)	9.7 ± 1.0	7.7 ± 0.6	9.4 ± 1.0	3.9 ± 0.7	1.4 ± 0.2	8.4 ± 0.7
Difference	−10% ($P=0.05$)	−14% ($P=0.04$)	+ 25% ($P=0.03$)	+ 5% ($P=0.66$)	−4% ($P=0.49$)	+ 4% ($P=0.95$)

V_{TCA}, total TCA cycle rate; V_{TCAn}, neuronal TCA cycle rate; V_{TCAg}, glial TCA cycle rate; V_{cycle}, glutamate–glutamine cycle rate; V_{TCAg}/V_{TCA}, astroglial contribution to total brain oxidative energy synthesis (in %); V_{cycle}/V_{TCAn}, ratio of the glutamate–glutamine cycle rate to neuronal TCA cycle rate ratio. B: NAA, *N*-acetylaspartate; Glu, glutamate; Ins, myo-inositol; Gln, glutamine; Cho, choline; Cr, creatine; flux values are expressed as μmol per g per min, whereas metabolite concentrations are expressed as μmol per g. Level of significance: *P*-values were calculated with a Bonferroni's *t*-test.

stimulation, subjects were asked to remain awake with their eyes open and to watch a slide show presentation during the study. A nurse was present at all times and performed periodic checks to insure that the subject was awake and observing the slides. Subjects were allowed to wear glasses within the magnet to view the projection screen.

Before the MRS studies, we carried out MRI volumetric analyses using T_1 image segmentation of the volume of interest of each volunteer. Figure 1 shows segmented (gray, white, CSF) MRI images of young and elderly subjects from each respective group. The percentage of gray matter versus gray + white matter in the volume of interest was similar in

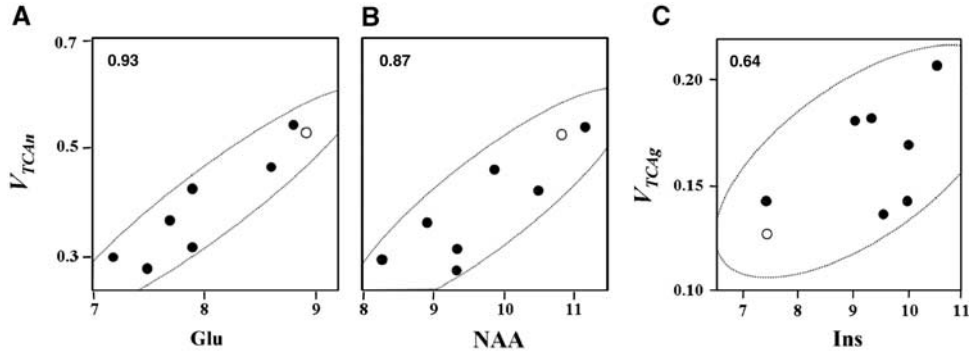

Figure 3 Pearson's correlation coefficients. (**A** and **B**) calculated between neuronal metabolites Glu and NAA and V_{TCAn}, neuronal TCA cycle rate; (**C**) calculated between astroglial metabolite Ins and V_{TCAg}, glial TCA cycle rate. Closed circles: individual values measured for Elderly ($n = 7$). Open circles: average values for the respective metabolite concentrations from a young cohort ($n = 7$). Fluxes and metabolite concentrations are expressed as μmol per g per min, and μmol per g, respectively.

Table 2 ^{13}C fractional enrichment of glutamate (from [1-^{13}C]glucose infusion) and glutamine (from [2-^{13}C]acetate infusion) in positions C4 and C3 for 'Young' and 'Elderly' subjects at the end of a 2-h infusion

(Mean ± s.d.)	*Glu-C4*	*Glu-C3*	*Gln-C4*	*Gln-C3*
Young ($n = 8$)	18.3 ± 1.2	13.6 ± 0.8	14.9 ± 2.4	6.8 ± 1.0
Elderly ($n = 7$)	17.3 ± 1.1	12.7 ± 0.9	15.0 ± 3.2	7.8 ± 1.5

Fractional enrichment values are given in %, (means ± s.d., $n = 7$ for 'Elderly' subjects; $n = 8$ for 'Young' subjects). The natural abundance (1.1%) was subtracted.

the young (47 ± 1%, $n = 8$) and elderly (49 ± 2%, $n = 7$) subjects. However, the percentage of CSF relative to the total volume was slightly higher in the aged group (elderly versus young: 18 ± 2% versus 15 ± 1%, mean ± s.d.

Figure 2 depicts the experimental time courses of glutamate-C4 and glutamate-C3 (from [1-^{13}C]glucose infusion) and glutamine-C4 and glutamine-C3 (from [2-^{13}C]acetate infusion) obtained for a 'Young' and an 'Elderly' volunteer. The slower rate of ^{13}C labeling of glutamate from [1-^{13}C]glucose in the elderly compared with the young subject is visually apparent from the time courses. The corresponding best fits of the metabolic model to the time courses yields values for the metabolic rates. The average values of the rates $\boldsymbol{V_{TCA}}$, V_{TCAn}, V_{TCAg}, and V_{cycle}, for both groups are given in Table 1. The steady-state ^{13}C fractional enrichments were similar in both the groups (see Table 2), indicating that the slower increase of labeling in the elderly subjects was due to a reduced rate in metabolism as opposed to a reduction in cell number.

As summarized in Table 1 and as shown schematically in Figure 4, there was a 28% reduction in neuronal mitochondrial TCA cycle flux (V_{TCAn}) in the elderly volunteers compared with the young volunteers. A similar decrease in mitochondrial TCA cycle flux (V_{cycle}) and rates of neuronal mitochondrial TCA cycle flux (V_{TCAn}) is consistent with findings in animal models showing that the glutamate–glutamine cycle flux (V_{cycle}) is proportional to mitochondrial energy metabolism (Sibson *et al*, 1998; Hyder *et al*, 2006). In addition to reduced rates of neuronal metabolism, we found evidence for altered glial mitochondrial metabolism in elderly subjects (Table 1). An increase in the relative labeling of glutamine-C3 to glutamine-C4 may reflect a larger fraction of the ^{13}C-labeled carbon that enters the glial TCA cycle from [2-^{13}C]acetate undergoing more than one turn relative to glutamine synthesis, which removes carbon from the TCA cycle (Lebon *et al*, 2002). Metabolic modeling of the labeling time courses indicated that astroglial TCA cycle rate (V_{TCAg}) was ~30% greater in the elderly subjects, all exceeding the average rate of the young subjects. As discussed below, a caveat to this interpretation is that the change in the glutamine relative C4 and C3 labeling may reflect a decrease in the relative rate of anaplerosis in the elderly subjects.

To test whether the changes in metabolic rates were a consequence of cellular alterations as opposed to differences in occipital lobe activation in the magnet, we compared the neuronal TCA cycle rates of each elderly subject with the concentrations of NAA and glutamate measured in the same volume using short TE ^{1}H MRS. *N*-acetylaspartate is synthesized in the neuronal mitochondria, and decreased levels observed in neurologic disorders correlate with either neuronal loss or reductions in neuronal functional activity (Moffett *et al*, 2007; Benarroch, 2008). Central nervous system glutamate is primarily found in glutamatergic neurons, and levels correlate with NAA. As illustrated in Figure 3, positive correlations were found between individual rates of neuronal mitochondrial TCA cycle flux (V_{TCAn}) and concentrations of the neuronal metabolites, NAA and glutamate (Pearson's correlations: $R = 0.87$ between NAA and V_{TCAn} and $R = 0.93$ between glutamate and V_{TCAn}). A similar relationship between neuronal oxidation rate and NAA levels was found by Lin

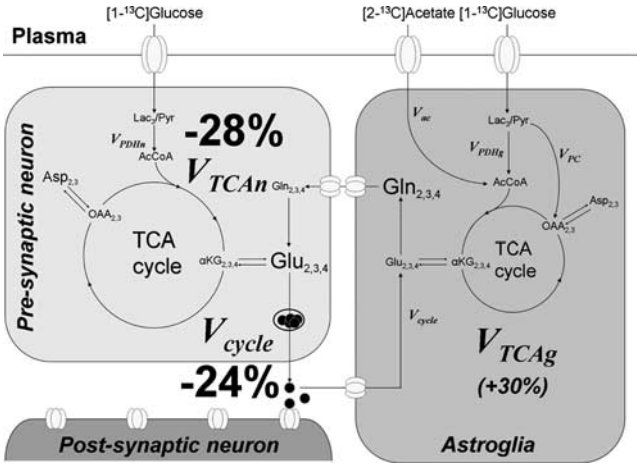

Figure 4 Neuronal-astroglial metabolic model and fluxes altered with aging. ^{13}C label that is incorporated from [2-^{13}C]acetate or [1-^{13}C]glucose enters the mitochondrial TCA cycle of astroglia and neurons (primarily), respectively. The exchange of label into the glutamine pool that is localized to the astroglia and the glutamate pool that is primarily neuronal allows the rates of the astroglial and neuronal TCA cycles to be measured. Label will cross from the neurons to the astroglia and back through the glutamate–glutamine cycle in which released neurotransmitter glutamate is taken up by the astroglia, converted to glutamine, and then released back to the neuron for restoration of the glutamate pool. We found that both the neuronal TCA cycle and the glutamate–glutamine cycle were reduced, and that the astroglial TCA cycle was increased in healthy elderly subjects. The primary findings are a decrease in both V_{cycle} and V_{TCAn} in the elderly subjects. There was also a measured increase in the rate of the glial TCA cycle in the elderly subjects; however, we have placed it in parentheses because of the possibility of other changes in glial metabolic pathways accounting for the difference in labeling patterns, in particular anaplerosis. Left: neuronal compartment; Right: astroglial compartment. Abbreviations: Lac, lactate; Glc, glucose; Pyr, pyruvate; AcCoA, acetyl coenzyme A; OAA, oxaloacetate; αKG, α-ketoglutarate; Glu, glutamate; Gln, glutamine; *Asp*, aspartate; V_{ac}, acetate consumption rate; V_{PDHn}, flux through neuronal pyruvate dehydrogenase; V_{PDHg}, astroglial flux through the pyruvate dehydrogenase; V_{TCAn}, neuronal TCA cycle rate; V_{TCAg}, glial TCA cycle rate; V_{PC}, flux through pyruvate carboxylase; V_{cycle}, glutamate–glutamine cycle rate.

et al (2003) in a ^{13}C MRS study of patients with Alzheimer's disease. The rate of the glial TCA cycle was compared with the level of myo-inositol, an osmolyte and putative glial cell marker (although the assignment is not well established as for NAA in neurons—see Martin, 2007), and a weaker but significant correlation was found (Pearson's $R = 0.64$).

Discussion

To examine whether aging affects brain mitochondrial function, we conducted two separate studies using [1-^{13}C]glucose and [2-^{13}C]acetate to specifically assess rates of the neuronal and glial TCA cycle flux, respectively, in healthy young and elderly subjects. We found that in elderly subjects, the rate of the neuronal TCA cycle was ~28% lower with a similar reduction in the rate of the glutamate–glutamine cycle. Before our study, age-related changes in brain metabolism in humans were reported using PET and arterio venous (AV) difference studies. Early AV difference studies by Kety (1956) reported an overall decrease in brain oxygen consumption ($CMRO_2$) with aging, which were supported by several $^{15}H_2O$-PET studies (Martin *et al*, 1991). Similarly, results of ^{18}F-fluoro-deoxy-glucose (^{18}FDG)-PET studies have noted reductions in overall brain glucose consumption (CMR_{glc}) with normal aging of ~10% to 20%, including the regions measured in this study (Kalpouzos *et al*, 2009). However, in contrast to the ^{13}C MRS methods used in the current studies, ^{18}FDG-PET studies do not directly assess neuronal and glial mitochondrial metabolism. Furthermore, conclusions regarding reduced CMR_{glc} have been questioned by Rapoport *et al.* who suggested that these differences could be accounted for by cortical shrinkage (Ibáñez *et al*, 2006).

An advantage of ^{13}C MRS is that both total metabolic flux and the turnover time of metabolic pools can be determined, permitting rate changes due to neuronal metabolism to be distinguished from potential neuronal loss. The turnover time, which is inversely proportional to the average metabolic flux within the cells, is not influenced by a loss of neurons. For example, assuming that oxidative metabolism in the remaining neurons is unaffected by lost cells, the turnover time of the ^{13}C label in glutamate would be the same as for a brain with no neuron loss. We found that the reduction in the neuronal TCA cycle rate reflected a slower turnover time (Figure 4) and could not be explained by tissue loss, as assessed by either quantitative volumetric MRI or by decreases in the absolute size of metabolite pools, which were significantly less (−10% and −14% for NAA and Glu, respectively) than the decrease in the neuronal TCA cycle rate.

Greater metabolic decreases in glucose utilization have been measured in humans with neurodegenerative diseases, such as Alzheimers's by PET (Rapoport, 1999) and ^{13}C MRS (Lin *et al*, 2003), but these changes are associated with a much greater extent of gray matter loss and tissue shrinkage than what was observed in our subjects. A potential explanation for the discrepancies in the FDG-PET literature on the basis of our findings is that the decrease in neuronal glucose oxidation may be masked by the increase in glial glucose oxidation, the degree of which may depends on the exact conditions in the scanner (e.g., degree of light and auditory deprivation, and wakefulness of the subject). Alternatively, because FDG-PET measures total glucose uptake, and not glycolysis, a selective decrease in the rate of the neuronal TCA cycle

may be masked by an increase in nonoxidative glycolysis.

The occipital volume of interest was chosen largely because the majority of ^{13}C MRS studies of the human brain have been reported from this region mainly because of the relative ease of acquiring MRS spectra from this site. However ^{13}C MRS spectra from the human frontal lobe has been recently shown (Sailasuta *et al*, 2008) opening up other brain regions to study. Both the elderly and young subject groups underwent stringent selection criteria to rule out conditions other than aging that may impact brain metabolism. Among the exclusion criteria were the use of medications, all chronic diseases including neurologic and psychiatric diseases, and acute disease at the time of the study. Tests for diabetes and hypertension were conducted to ensure that our subject groups were free of these conditions, the latter being found by Salat *et al* (2004) to have the major impact on CMR_{glc} with aging. Undiagnosed depression was not tested, but although an early preliminary PET study reported significant metabolic decline in depressed older subjects (Kumar *et al*, 1993), subsequent studies have found only small metabolic changes (Nikolaus *et al*, 2000) and the earlier finding may have been due to a history of hypertension and vascular disease not being excluded (Ibáñez *et al*, 2006). The possibility of undiagnosed Alzheimer's disease and other neurodegenerative or ischemic disorders were ruled out on the basis of examination of the quantitative T_1 segmentation image, which showed no evidence of significant gray matter changes or previous lesions. Mild cognitive impairment due to incipient Alzheimer's disease, which could have been missed does not significantly affect the metabolic rate of the midline occipital lobe (Rapoport, 1999). Owing to the difficulty of finding elderly subjects who met all these exclusion criteria, and the rigors of the 2.5-h study, our subject group number was somewhat limited. Further advances in ^{13}C MRS may allow the same information to be obtained from studies with reduced infusion times (Lin *et al*, 2003).

An alternate explanation for the reduction in V_{TCAn} and V_{cycle} is that the elderly subjects had reduced occipital lobe activity because of different levels of wakefulness within the magnet. To minimize these differences, subjects were regularly questioned by the nurse present during the study to insure that they were awake. Furthermore, the strong correlation between the concentration of NAA and the reduction in V_{TCAn} suggests that the reduction in neuronal mitochondrial activity in the elderly subjects reflects a chronic condition rather than an acute effect of wakefulness. Studies in animal models and in human clinical diseases, such as epilepsy and multiple sclerosis, have shown that when average neuronal activity is reduced because of a reduction in neuronal input (e.g., diaschisis), NAA levels are also decreased, and that normal NAA levels are restored once activity is normalized (De Stefano *et al*, 1999; Moffett *et al*, 2007; Benarroch, 2008). This relationship with activity is most likely due to NAA being synthesized in the neuronal mitochondria. Isolated cell studies have shown a direct relationship between the rates of NAA synthesis and mitochondrial oxygen consumption (Clark *et al*, 2006).

Although functional alterations in the aged brain are well established, the reported changes in cortical cellular composition and density in humans with healthy aging are relatively minor (Peinado, 1998). There are small reductions in gray and white matter volume with the most pronounced reductions in cortical thickness occurring in the frontal regions (Resnick *et al*, 2003). A relatively minimal loss of volume has been reported in the occipital and occipital–parietal lobe, consistent with our segmentation findings (Haug and Eggers, 1991; Leuba and Kraftsik, 1994). The number and density of neuronal and glia cells have also been reported to be unchanged in most of the cortical areas of the aged human brain (Haug and Eggers, 1991).

An alternate explanation for reduced neuronal mitochondrial metabolism, and reports of reduced brain function with healthy aging, is that it reflects impaired mitochondrial metabolic capacity. Theoretical studies (Attwell and Laughlin, 2001) have concluded that functional processes account for the majority of energy consumption even in the resting state in rodents and humans. Consistent with this conclusion, MRS measurements in animal models have found a direct proportionality between the rate of the neuronal TCA cycle and the rate of the glutamate–glutamine cycle, and that functional processes account for more than 80% of neuronal energy consumption in the awake rodent cerebral cortex (Sibson *et al*, 1998; Oz *et al*, 2004; for a review, see Hyder *et al*, 2006). In this study, the decrease in V_{cycle} was similar in proportion to the decrease in V_{TCAn} (see Table 1 and Figure 4: -24% and -28% for V_{cycle} and V_{TCAn}, respectively) as found in the rodent studies, which supports a similar relationship between neuronal function and mitochondrial energy production in the human brain. The proportional decrease is consistent with a reduction in mitochondrial capacity resulting in reduced function (as measured by the glutamate–glutamine cycle). However, at present, we cannot rule out the converse, namely that reduced neuronal activity leads to a proportional reduction in neuronal mitochondrial metabolism. Studies examining the capacity of the aged brain to sustain increased rates of mitochondrial metabolism at graded levels of functional stimulation may distinguish these possibilities.

Our metabolic analysis indicated an increase in the glial TCA cycle in the elderly subjects. In the modeling analysis, this difference was largely caused by a greater labeling of glutamine-C3 relative to glutamine-C4 during [2-^{13}C]acetate infusion between elderly and young subjects, indicating that glial mitochondrial metabolism is also altered with aging. However, altered rates of other metabolic pathways

associated with glial mitochondrial metabolism could influence the relative ^{13}C labeling of glutamine-C3 and glutamine-C4. For example, reduced oxaloacetate synthesis from pyruvate (synthesized from unlabeled glucose) and CO_2 catalyzed by astroglial enzyme, pyruvate carboxylase, would lead to a relative increase in α-ketoglutarate (and glutamine) C3 to C4 labeling. An aging-related decline in the rate of anaplerosis could lead to decreased neuronal glutamate, as was seen. However, the lack of significant changes in glutamine levels (also expected to be lower) was not observed. Further studies using pathway-specific ^{13}C-labeled substrates, e.g., [2-^{13}C]glucose (Mason *et al*, 2007), are required to address this question. Further evidence supporting the finding of altered glial metabolism was the relationship between V_{TCAg} and the level of myo-inositol in the elderly subjects, which has been proposed to be a marker for altered glial function (although not completely specific to glia) and is known to change in level in neurodegenerative disorders (for a review, see Martin, 2007). In nonhuman primates, there is subtle evidence for decreased neuronal and increased astroglia volume, although as reported for the human brain, the differences are not uniform throughout the brain, and not nearly to the extent as in the rodent brain (Peters, 2002; Duan *et al*, 2003).

Mitochondrial dysfunction associated with aging has been suggested to be caused by an accumulation of mtDNA defects and an increased production of reactive oxygen species (Cooper *et al*, 1992; Kujoth *et al*, 2005). The mitochondrial electron transport chain is responsible for the transfer of electrons from NADH or FADH, to electron acceptors, and to oxygen, forming H_2O. These biochemical events may lead to a small amount (1% to 5%) of electron leakage and, subsequently, to reactive oxygen species production. The brain is not the sole organ where oxidative stress may lead to altered mitochondrial capacity. Indeed, reduced mitochondrial energy production *in vivo* with aging has also been shown in human skeletal muscle using MRS (Petersen *et al*, 2003). Whether a decline in mitochondrial capacity in healthy aging is a consequence of reactive oxygen species production or other factors cannot be addressed herein and awaits future studies.

In conclusion, our results show that healthy aging is associated with a reduction in brain cortical neuronal mitochondrial energy production and altered glial mitochondrial metabolism. The reductions in neuronal mitochondrial metabolism, possibly secondary to a loss of mitochondrial capacity, may in part be responsible for the decline in brain function associated with healthy aging.

Conflict of interest

The authors declare no conflict of interest.

Acknowledgements

The authors thank Mikhail Smolgovsky, Yanna Kosover, Donna D'Eugenio, RN, Gina D'Agostino, RN, and the Yale/New Haven Hospital General Clinical Research Center for their technical assistance; Terry Nixon and Scott McIntyre for maintenance and upgrades to the MRS system; Peter Brown for design and construction of the radiofrequency probes, and the volunteers for their participation in these studies; and Dr Susan Fitzpatrick for helpful discussions regarding neuroanatomical and metabolic changes with aging.

References

Attwell D, Laughlin SB (2001) An energy budget for signaling in the grey matter of the brain. *J Cereb Blood Flow Metab* 21:1133–45

Barker PB, Breiter SN, Soher BJ, Chatham JC, Forder JR, Samphilipo MA, Magee CA, Anderson JH (1994) Quantitative proton spectroscopy of canine brain: in vivo and in vitro correlations. *Magn Reson Med* 32: 157–63

Behar KL, Rothman DL, Spencer DD, Petroff OA (1994) Analysis of macromolecule resonances in 1H NMR spectra of human brain. *Magn Reson Med* 32: 294–302

Benarroch EE (2008) N-acetylaspartate and N-acetylaspartylglutamate: neurobiology and clinical significance. *Neurology* 70:1353–7

Clark JF, Doepke A, Filosa JA, Wardle RL, Lu A, Meeker TJ, Pyne-Geithman GJ (2006) N-acetylaspartate as a reservoir for glutamate. *Med Hypotheses* 67:506–12

Cooper JM, Mann VM, Schapira AH (1992) Analyses of mitochondrial respiratory chain function and mitochondrial DNA deletion in human skeletal muscle: effect of ageing. *J Neurol Sci* 113:91–8

De Stefano N, Narayanan S, Matthews PM, Francis GS, Antel JP, Arnold DL (1999) In vivo evidence for axonal dysfunction remote from focal cerebral demyelination of the type seen in multiple sclerosis. *Brain* 122:1933–9

Duan H, Wearne SL, Rocher AB, Macedo A, Morrison JH, Hof PR (2003) Age-related dendritic and spine changes in corticocortically projecting neurons in macaque monkeys. *Cereb Cortex* 13:950–61

Govindaraju V, Young K, Maudsley AA (2000) Proton NMR chemical shifts and coupling constants for brain metabolites. *NMR Biomed* 13:129–53

Gruetter R, Seaquist ER, Uğurbil K (2001) A mathematical model of compartmentalized neurotransmitter metabolism in the human brain. *Am J Physiol Endocrinol Metab* 281:E100–12

Haug H, Eggers R (1991) Morphometry of the human cortex cerebral and corpus striatum during aging. *Neurobiol Aging* 12:336–8; discussion 352–335

Hedden T, Gabrieli JD (2004) Insights into the ageing mind: a view from cognitive neuroscience. *Nat Rev Neurosci* 5:87–96

Henry PG, Oz G, Provencher S, Gruetter R (2003) Toward dynamic isotopomer analysis in the rat brain in vivo: automatic quantitation of 13C NMR spectra using LCModel. *NMR Biomed* 16:400–12

Henry PG, Adriany G, Deelchand D, Gruetter R, Marjanska M, Oz G, Seaquist ER, Shestov A, Uğurbil K (2006) In vivo 13C NMR spectroscopy and metabolic modeling in the brain: a practical perspective. *Magn Reson Imaging* 24:527–39

Hyder F, Patel AB, Gjedde A, Rothman DL, Behar KL, Shulman RG (2006) Neuronal-glial glucose oxidation and glutamatergic-GABAergic function. *J Cereb Blood Flow Metab* 26:865–77

Ibáñez V, Pietrini P, Furey ML, Alexander GE, Millet P, Bokde AL, Teichberg D, Schapiro MB, Horwitz B, Rapoport SI (2006) Resting state brain glucose metabolism is not reduced in normotensive healthy men during aging, after correction for brain atrophy. *Brain Res Bull* 63:147–54

Kalpouzos G, Chetelat G, Baron JC, Landeau B, Mevel K, Godeau C, Barre L, Constans JM, Viader F, Eustache F, Desgranges B (2009) Voxel-based mapping of brain gray matter volume and glucose metabolism profiles in normal aging. *Neurobiol Aging* 30:112–24

Kety SS (1956) Human cerebral blood flow and oxygen consumption as related to aging. *J Chronic Dis* 3:478–86

Kujoth GC, Hiona A, Pugh TD, Someya S, Panzer K, Wohlgemuth SE, Hofer T, Seo AY, Sullivan R, Jobling WA, Morrow JD, Van Remmen H, Sedivy JM, Yamasoba T, Tanokura M, Weindruch R, Leeuwenburgh C, Prolla TA (2005) Mitochondrial DNA mutations, oxidative stress, and apoptosis in mammalian aging. *Science* 309:481–4

Kumar A, Newberg A, Alavi A, Berlin J, Smith R, Reivich M (1993) Regional cerebral glucose metabolism in late-life depression and Alzheimer disease: a preliminary positron emission tomography study. *Proc Natl Acad Sci USA* 90:7012–9

Lebon V, Petersen KF, Cline GW, Shen J, Mason GF, Dufour S, Behar KL, Shulman GI, Rothman DL (2002) Astroglial contribution to brain energy metabolism in humans revealed by 13C nuclear magnetic resonance spectroscopy: elucidation of the dominant pathway for neurotransmitter glutamate repletion and measurement of astrocytic oxidative metabolism. *J Neurosci* 22: 1523–31

Lentner C (1981) *Geigy Scientific Tables*. Basel, Switzerland: Ciba-Geigy, pp 222

Leuba G, Kraftsik R (1994) Changes in volume, surface estimate, three-dimensional shape and total number of neurons of the human primary visual cortex from midgestation until old age. *Anat Embryol (Berl)* 190:351–66

Lin AP, Shic F, Enriquez C, Ross BD (2003) Reduced glutamate neurotransmission in patients with Alzheimer's disease—an in vivo 13C magnetic resonance spectroscopy study. *MAGMA* 16:29–42

Mangia S, Giove F, Tkác I, Logothetis NK, Henry PG, Olman CA, Maraviglia B, Di Salle F, Uğurbil K (2009) Metabolic and hemodynamic events after changes in neuronal activity: current hypotheses, theoretical predictions and *in vivo* NMR experimental findings. *J Cereb Blood Flow Metab* 29:441–63

Marjanska M, Henry P-G, Gruetter R, Garwood M, Uğurbil K (2004) A new method for proton detected carbon edited spectroscopy using LASER. In: Proceedings of the 12th ISMRM meeting (Kyoto, Japan). p. 679

Martin AJ, Friston KJ, Colebatch JG, Frackowiak RS (1991) Decreases in regional cerebral blood flow with normal aging. *J Cereb Blood Flow Metab* 11:684–9

Martin WR (2007) MR spectroscopy in neurodegenerative disease. *Mol Imaging Biol* 9:196–203

Mason GF, Gruetter R, Rothman DL, Behar KL, Shulman RG, Novotny EJ (1995) Simultaneous determination of the rates of the TCA cycle, glucose utilization, alpha-ketoglutarate/glutamate exchange, and glutamine synthesis in human brain by NMR. *J Cereb Blood Flow Metab* 15:12–25

Mason GF, Pan JW, Chu WJ, Newcomer BR, Zhang Y, Orr R, Hetherington HP (1999) Measurement of the tricarboxylic acid cycle rate in human grey and white matter in vivo by 1H-[13C] magnetic resonance spectroscopy at 4.1T. *J Cereb Blood Flow Metab* 19:1179–88

Mason GF, Rothman DL (2002) Graded image segmentation of brain tissue in the presence of inhomogeneous radio frequency fields. *Magn Reson Imaging* 20:431–6

Mason GF (2003) Magnetic resonance spectroscopy for studies of neurotransmission *in vivo*. *Psychopharmacol Bull* 37:26–40

Mason GF, Petersen KF, de Graaf RA, Shulman GI, Rothman DL (2007) Measurements of the anaplerotic rate in the human cerebral cortex using 13C magnetic resonance spectroscopy and [1-13C] and [2-13C] glucose. *J Neurochem* 100:73–86

Moffett JR, Ross B, Arun P, Madhavarao CN, Namboodiri AM (2007) N-Acetylaspartate in the CNS: from neurodiagnostics to neurobiology. *Prog Neurobiol* 81:89–131

Nikolaus S, Larisch R, Beu M, Vosberg H, Muller-Gartner HW (2000) Diffuse cortical reduction of neuronal activity in unipolar major depression: a retrospective analysis of 337 patients and 321 controls. *Nucl Med Commun* 21:1119–25

Oz G, Berkich DA, Henry PG, Xu Y, LaNoue K, Hutson SM, Gruetter R (2004) Neuroglial metabolism in the awake rat brain: CO2 fixation increases with brain activity. *J Neurosci* 24:11273–9

Peinado MA (1998) Histology and histochemistry of the aging cerebral cortex: an overview. *Microsc Res Tech* 43:1–7

Peters A (2002) Structural changes that occur during normal aging of primate cerebral hemispheres. *Neurosci Biobehav Rev* 26:733–41

Petersen KF, Befroy D, Dufour S, Dziura J, Ariyan C, Rothman DL, DiPietro L, Cline GW, Shulman GI (2003) Mitochondrial dysfunction in the elderly: possible role in insulin resistance. *Science* 300:1140–2

Provencher SW (1993) Estimation of metabolite concentrations from localized in vivo proton NMR spectra. *Magn Reson Med* 30:672–9

Rapoport SI (1999) Functional brain imaging in the resting state and during activation in Alzheimer's disease. Implications for disease mechanisms involving oxidative phosphorylation. *Ann NY Acad Sci* 893:138–53

Reddy PH (2007) Mitochondrial dysfunction in aging and Alzheimer's disease: strategies to protect neurons. *Antioxid Redox Signal* 9:1647–58

Resnick SM, Pham DL, Kraut MA, Zonderman AB, Davatzikos C (2003) Longitudinal magnetic resonance imaging studies of older adults: a shrinking brain. *J Neurosci* 23:3295–301

Sailasuta S, Robertson LW, Harris KC, Gropman AL, Allen PS, Ross BD (2008) Clinical NOE 13C MRS for neuropsychiatric disorders of the frontal lobe. *J Magn Reson* 195:219–25

Salat DH, Buckner RL, Snyder AZ, Greve DN, Desikan RS, Busa E, Morris JC, Dale AM, Fischl B (2004) Thinning of the cerebral cortex in aging. *Cereb Cortex* 14:721–30

Shen J, Rothman DL (2002) Magnetic resonance spectroscopic approaches to studying neuronal: glial interactions. *Biol Psychiatry* 52:694–700

Shen J, Petersen KF, Behar KL, Brown P, Nixon TW, Mason GF, Petroff OA, Shulman GI, Shulman RG, Rothman DL (1999) Determination of the rate of the glutamate/glutamine cycle in the human brain by in vivo 13C NMR. *Proc Natl Acad Sci USA* 96:8235–40

Shen J, Rothman DL, Behar KL, Xu S (2009) Determination of the glutamate-glutamine cycling flux using two-compartment dynamic metabolic modeling is sensitive to astroglial dilution. *J Cereb Blood Flow Metab* 29:108–18

Shestov AA, Valette J, Uğurbil K, Henry PG (2007) On the reliability of 13C metabolic modeling with two-compartment neuronal-glial models. *J Neurosci Res* 85:3294–303

Sibson NR, Dhankhar A, Mason GF, Rothman DL, Behar KL, Shulman RG (1998) Stoichiometric coupling of brain glucose metabolism and glutamatergic neuronal activity. *Proc Natl Acad Sci USA* 95:316–21

Supplementary Information accompanies the paper on the Journal of Cerebral Blood Flow & Metabolism website (http://www.nature.com/jcbfm)